



OPEN BRD4 as the key lactylation related gene in heart failure identified through bioinformatics analysis

Kaiyuan Li^{1,2,4}, Lingyu Han^{2,4}, Xiaowen Wang^{3,4}, Zhipeng Zheng², Min Sha², Jun Ye^{1,2}✉ & Li Zhu^{1,2}✉

Lactylation modification is postulated to influence the progression of heart failure (HF) through diverse pathways, albeit the underlying mechanisms remain elusive. Methods In this study, bioinformatics approaches were employed to analyze the HF dataset (GSE5406) retrieved from the Gene Expression Omnibus, with the objective of identifying lactylation-related genes (LRGs). Key LRGs implicated in HF were selected using the Least Absolute Shrinkage and Selection Operator (LASSO) and Weighted Gene Co-Expression Network Analysis (WGCNA). The diagnostic efficacy and biological significance of these genes were evaluated through receiver operating characteristic (ROC) curve analysis, Gene Set Enrichment Analysis, and immune cell infiltration analysis. Furthermore, the findings were validated using single-cell sequencing datasets (GSE161470) and in vitro cell models to ascertain the expression patterns and functional roles of the identified key LRGs. A total of 276 LRGs were identified from the HF dataset. Initial screening utilizing two bioinformatics analysis methods pinpointed BRD4 as a potential pivotal LRG influencing HF progression. ROC analysis revealed a high diagnostic accuracy for BRD4, with an Area Under the Curve score of 0.877. Immune cell infiltration and single-cell data analyses indicated that BRD4 exhibits a strong association with immune cells, including mast cells, T cells, and macrophages, and demonstrates significantly elevated expression in these immune cells as well as in cardiomyocytes. Both BRD4 mRNA and protein levels were found to be upregulated compared to control groups. This study represents the first to utilize multiple bioinformatics analysis methods to identify BRD4 as a key LRG in HF, thereby establishing a foundation for future investigations into acylation-related mechanisms in HF.

Keywords Heart failure, Lactylation, LASSO, WGCNA, BRD4

Heart failure (HF) is a complex clinical syndrome characterized by the heart's inability to pump sufficient blood to meet the body's metabolic demands^{1,2}. The underlying pathophysiology includes myocardial injury, hemodynamic changes, neurohormonal activation, and inflammatory responses^{3,4}. Despite significant advances in the management and treatment of HF, understanding its molecular mechanisms is crucial for developing new therapeutic strategies.

Lactylation is a critical post-translational modification that plays a key role in regulating protein and cellular functions^{5,6}. Existing studies indicate that lactylation of certain genes may influence the risk of various cardiac diseases and potentially impact disease progression by modulating cellular metabolism and immune responses^{7,8}. For example, studies have shown that lactylation plays a critical role in cardiomyocyte apoptosis following myocardial infarction, with increased lactylation levels closely associated with the extent of myocardial damage⁹. Additionally, lactylation has been implicated in atherosclerosis, significantly influencing the functions of vascular smooth muscle cells and macrophages^{10,11}. These findings suggest that lactylation may be pivotal in the pathogenesis of various cardiac diseases. However, the specific role and mechanisms of lactylation in HF remain largely unknown, necessitating further investigation into its potential impacts.

This study aims to explore the role of lactylation-related genes (LRGs) in HF using bioinformatics methods. By analyzing HF datasets from the Gene Expression Omnibus (GEO) database, we seek to identify LRGs associated with HF and employ machine learning techniques to pinpoint key genes (Fig. 1). The findings of this

¹Graduate School of Dalian Medical University, Dalian Medical University, Dalian 116000, Liaoning, P.R. China.

²Department of Cardiology, The Affiliated Taizhou People's Hospital of Nanjing Medical University, Taizhou 225300, Jiangsu, P.R. China. ³Nanjing University of Chinese Medicine, Nanjing 210000, P.R. China. ⁴Kaiyuan Li, Lingyu Han and Xiaowen Wang contributed equally. ✉email: dingyinglinyejun@126.com; tzheartchina@126.com

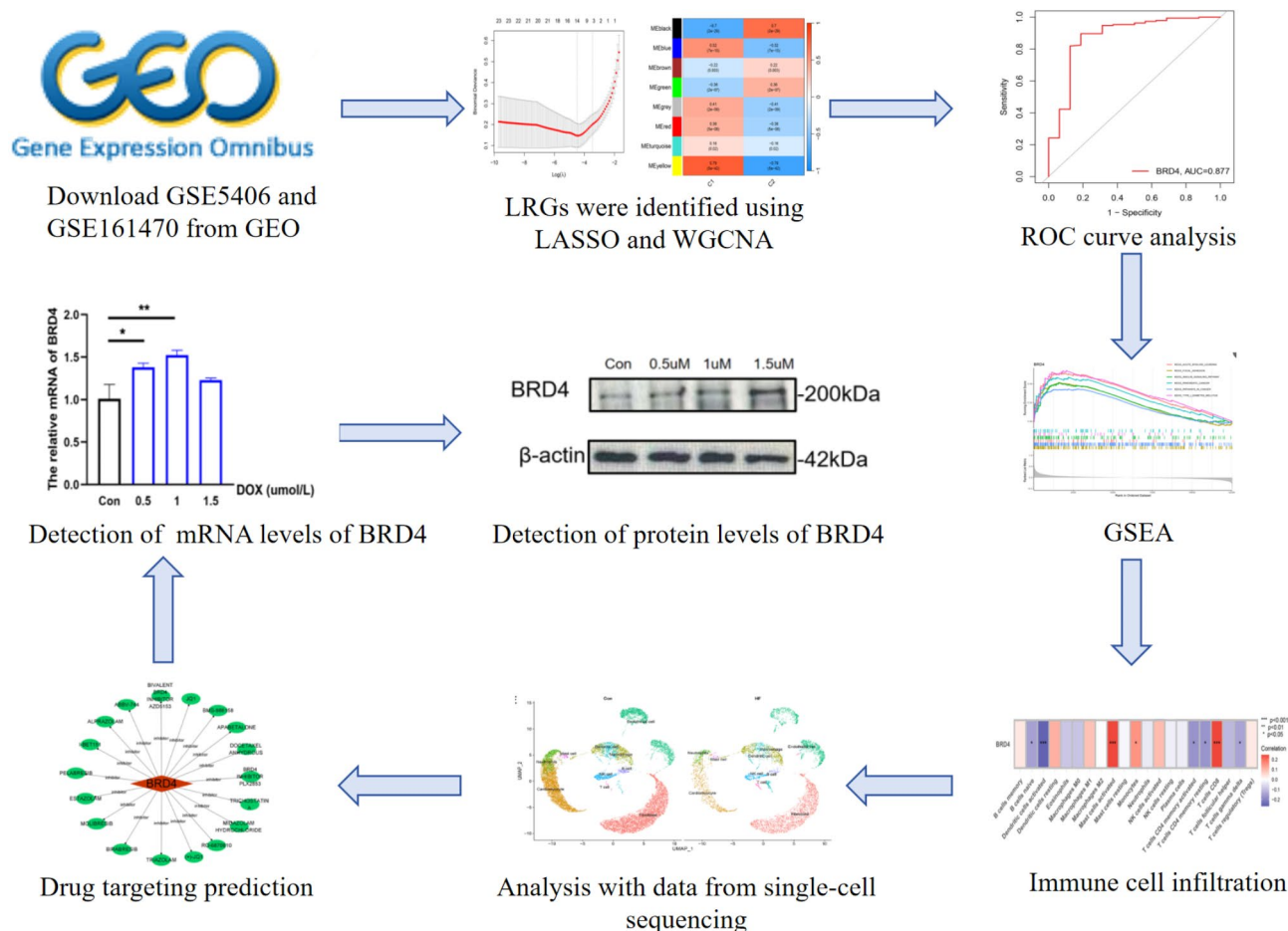


Fig. 1. Flowchart for the study.

study are expected to provide new insights into the role of lactylation in HF, revealing potential biomarkers and therapeutic targets to improve the diagnosis and treatment of HF.

Materials and methods

Identification and correlation analysis of key genes in HF

This study searched for gene expression profile datasets related to HF in the GEO database using the keyword 'heart failure'. Several HF datasets, including GSE76701, GSE57338, GSE5406, and GSE84796, were considered. The dataset with the largest sample size, GSE5406, was ultimately included in this study. To further analyze the data, we categorized the original dataset as follows: 'nonfailing LV myocardium' was set as the control group, while 'Ischemic and Idiopathic' were grouped as the HF group. Probes were annotated using the corresponding annotation file. Additionally, the single-cell dataset GSE161470 related to HF was retrieved. The data from the GEO database are public resources, and this study did not require additional ethical approval.

The 332 LRGs were curated from previous literature and cross-validated using the GeneCards database (<https://www.genecards.org/>) with the keyword 'lactylation' (Supplementary Table 1)^{12,13}. The final list was generated by combining experimentally validated lactylated proteins from human and murine studies. The 'limma' package was used to screen differentially expressed LRGs (DLRGs) ($P < 0.05$). Furthermore, heatmaps and correlation analysis plots were generated using the 'heatmap' and 'corrplot' packages, respectively, to visualize the results.

Gene ontology (GO) and Kyoto encyclopedia of genes genomes (KEGG) functional enrichment analysis

This study utilized the 'clusterProfiler' package to perform GO and KEGG functional enrichment analyses on differentially expressed mRNA¹⁴. The GO analysis comprised three main categories: molecular function (MF), cellular component (CC), and biological process (BP)¹⁵.

Screening DLRGs using least absolute shrinkage and selection operator (LASSO)

The 'glmnet' package in R was used to construct an optimal LASSO logistic regression model. Cross-validation was used to select the tuning parameter (λ) with the smallest mean squared error to build the optimal LASSO logistic regression model, thus effectively identifying DLRGs that are closely related to HF¹⁶.

Combined weighted gene Co-Expression network analysis (WGCNA) for analysis

WGCNA was utilized to assess gene expression correlations, clustering genes exhibiting similar expression patterns into distinct modules, and subsequently selecting the most significant module associated with the HF phenotype for in-depth analysis. This methodology facilitates the identification of gene modules that are linked to disease phenotypes, thereby enabling the exploration of potential functional genes and their associated biological pathways.

Analysis of receiver operating characteristic (ROC)

Genes obtained from both the LASSO and WGCNA were intersected using a Venn diagram to identify the intersecting genes, referred to as the key DLRGs. The 'pROC' package in R software was utilized to conduct ROC curve analysis, assessing the stability of the two algorithms and their sensitivity in diagnosing HF¹⁷. The area under curve (AUC) greater than 0.7 indicated favorable diagnostic performance.

Gene set enrichment analysis (GSEA) analysis

The GSEA is commonly used to analyze and interpret pathway-level changes in transcriptomic experiments, aiding in the investigation of underlying mechanisms. The 'clusterProfiler' package in R was utilized to perform GSEA, while the 'ggplot2' and 'enrichplot' packages were used for visualization¹⁸. A gene set was considered significant if it achieved an adjusted *P* value of less than 0.05.

Correlation between key DLRGs and infiltrating immune cells

This study used the CIBERSORT algorithm to calculate the proportion of 22 immune cells infiltrating the cardiac tissues of patients with HF, with the *P* value < 0.05 as the threshold of significance. Pearson correlation coefficient was used to analyze the relationship between key DLRGs and infiltrating immune cells.

Analysis of single-cell dataset

The Single-cell data (GSE161470) included left ventricular samples from 4 non-failing and 1 failing heart. The 'Seurat' R package was used for quality control and analysis of the single-cell dataset. Initially, sequencing depth and cell counts were assessed to remove low-quality single-cell data^{19,20}. The top 1500 highly variable genes were then extracted and subjected to Principal Component Analysis (PCA) for linear dimensionality reduction. Cells were clustered using the FindClusters function in Seurat with the Louvain algorithm, and marker genes for each cluster were identified. Cluster annotation was performed by integrating published literature, the CellMarker database, and the 'SingleR' R package. Marker genes for each cluster were defined as those showing the greatest differential expression in the principal components (PCs)^{21,22}.

Targeted drug prediction

This study utilized the DGIdb database to predict potential targeted drugs for key DLRGs. Based on the prediction results, a drug regulation network was constructed.

Construction of HF cell model

Doxorubicin (Dox, Sigma-Aldrich) was used in this study to construct a model of heart failure in cardiomyocytes^{23,24}. The AC16 cells were placed in a 37 °C, 5% CO₂ incubator. The cells were also divided into control and DOX groups (0.5 μmol/L, 1 μmol/L, 1.5 μmol/L, 2 μmol/L) to establish the model for subsequent experiments.

CCK-8 assay

The Cell viability was measured using the Cell Counting Kit-8 (CCK-8) according to the manufacturer's instructions. Cells were seeded into 96-well plates at a density of 5×10^3 cells per well. After treatment with 10 μL CCK-8 solution for the specified time, absorbance at 450 nm was measured after a 2-hour incubation in the dark.

RNA extraction, reverse transcription, and Real-time quantitative PCR (RT-qPCR)

Total RNA was extracted using the Trizol method, and RNA purity was assessed using a NanoDrop ND-1000 spectrophotometer to determine RNA concentration and quality. The extracted RNA was reverse transcribed using a reverse transcription kit, followed by fluorescence RT-qPCR using the SYBR Green method. The reaction system was 20 μL, with pre-denaturation at 95 °C for 1 min, denaturation at 95 °C for 15 s, renaturation at 60 °C for 20 s, and extension at 72 °C for 30 s, for a total of 40 cycles. GAPDH was used as the reference gene, with primer sequences shown in Table 1.

Western blot

Total cellular proteins were extracted and subsequently quantified. The protein samples were resolved by SDS-PAGE and then transferred onto PVDF membranes. The membranes were subsequently incubated with a primary antibody against BRD4 (Proteintech, catalog number 28486-1-AP, dilution 1:1000). The bands were visualized using chemiluminescence, and the expression levels of BRD4 were quantitatively analyzed using ImageJ software.

Statistical analysis

Data processing and analysis were conducted using GraphPad Prism 9 software. Statistical comparisons between groups were performed using an unpaired *t*-test, with a *P*-value less than 0.05 considered to be statistically significant.

Gene name	Preverseimereverse sequence (5' to 3')
hsa-BRD4-forward	CACCCAGCACCAGAGAAGAG
hsa-BRD4-reverse	CTCATGTCCATGGGGTGCTT
hsa-ANP-forward	AGCCCCCGCTTCTTCATTC
hsa-ANP-reverse	CAACGCAGACCTGATGGATT
hsa-BNP-forward	CACAGGTGTCTGGAAGTCCC
hsa-BNP-reverse	TAATGCCGCCTCAGCACTTT
hsa-GAPDH-forward	CCGTTGAATTTGCCGTGA
hsa-GAPDH-reverse	TGATGACCCTTTGGCTCCC

Table 1. Primer sequences.

Results

Identification of DLRGs

After merging and organizing the HF dataset (GSE5406), 95 DLRGs were screened, including 33 upregulated and 62 downregulated genes (Fig. 2A–B).

Functional enrichment analysis

GO and KEGG enrichment analyses were carried out on 95 DLRGs. In the BP category, DLRGs were predominantly implicated in mRNA processing, ribonucleoprotein complex biogenesis, among other functional roles. With regard to CC, DLRGs were localized to heterochromatin and various other cellular structures. MF analysis revealed associations with nucleosomal DNA binding and cadherin binding (Fig. 2C). The KEGG enrichment analysis indicated that DLRGs were primarily enriched in pathways related to carbon metabolism, the pentose phosphate pathway, and glycolysis/gluconeogenesis (Fig. 2D).

Identification of BRD4 as the key DLRG

The LASSO analysis identified 14 DLRGs (Fig. 2E–F) (Supplementary Table 2). To determine if potential gene modules were associated with HF, WGCNA was performed on all candidate genes (Fig. 2G). WGCNA identified 8 distinct modules, and positive correlation analysis revealed a significant association of the MEyellow module with HF, resulting in 37 key genes (Fig. 2H–I) (Supplementary Table 3). The intersection of genes identified by both machine learning methods revealed BRD4 as the potential key DLRG (Fig. 2J). ROC analysis showed that the BRD4 gene had an AUC score of 0.877 (95% CI: 0.9669–1.000), indicating high diagnostic accuracy and reliability (Fig. 3A). GSEA indicated that BRD4 was closely associated with pathways such as focal adhesion, pathways in cancer, and the acute insulin signaling pathway (Fig. 3B). The shape of the curve and the top markers highlighted the significant involvement of the BRD4 gene in these biological pathways.

Correlation analysis of BRD4 and immune cells

BRD4 was significantly negatively correlated with five immune cell types including dendritic cell activation. There was a significant positive correlation with three immune cells including mast cell activation ($P < 0.05$ for all). These findings provide new perspectives for understanding the role of BRD4 in immune regulation (Fig. 3C).

Distribution and expression of BRD4 in Single-Cell sequencing dataset

The single-cell dataset for HF, designated as GSE161470, was derived from a dataset uploaded in 2021. This dataset comprises samples from the left ventricles of four non-failing hearts and one failing heart. In this study, a clustering algorithm was employed to classify the cell types within the HF single-cell sequencing datasets into 25 distinct subgroups. The results were visualized using t-SNE (t-distributed Stochastic Neighbor Embedding) and UMAP (Uniform Manifold Approximation and Projection). The 'FindAllMarkers' function was utilized to identify DEGs within each cluster, with a log-fold change (logFC) threshold set at 0.25. Based on the top 10 subtype-specific DEGs, ten cell types were identified: B cells, cardiomyocytes, dendritic cells, endothelial cells, fibroblasts, macrophages, mast cells, neutrophils, NK cells, and T cells (Fig. 3D). BRD4 was found to be highly expressed in cardiomyocytes, macrophages, neutrophils, dendritic cells, T cells, and mast cells. In the HF group, BRD4 expression was significantly elevated in cardiomyocytes, dendritic cells, and T cells compared to the control group (Fig. 3E–F).

Targeted drug prediction

19 potential drugs targeting BRD4 were predicted using the DGIdb database. Among these, six drugs, including midazolam hydrochloride and estazolam, have been approved for the treatment of conditions such as seizures, atherosclerosis, and cancer (Fig. 3G). These predictions provide a proof-of-concept for the druggability of BRD4; however, rigorous pharmacological validation is necessary to rule out any harmful pleiotropic effects.

Successful construction of HF cell model

The AC16 cells were treated with different concentrations of DOX (0.5 $\mu\text{mol/L}$, 1 $\mu\text{mol/L}$, 1.5 $\mu\text{mol/L}$, and 2 $\mu\text{mol/L}$) to establish a HF cell model. Cell viability was assessed using the CCK8 assay. Results indicated a

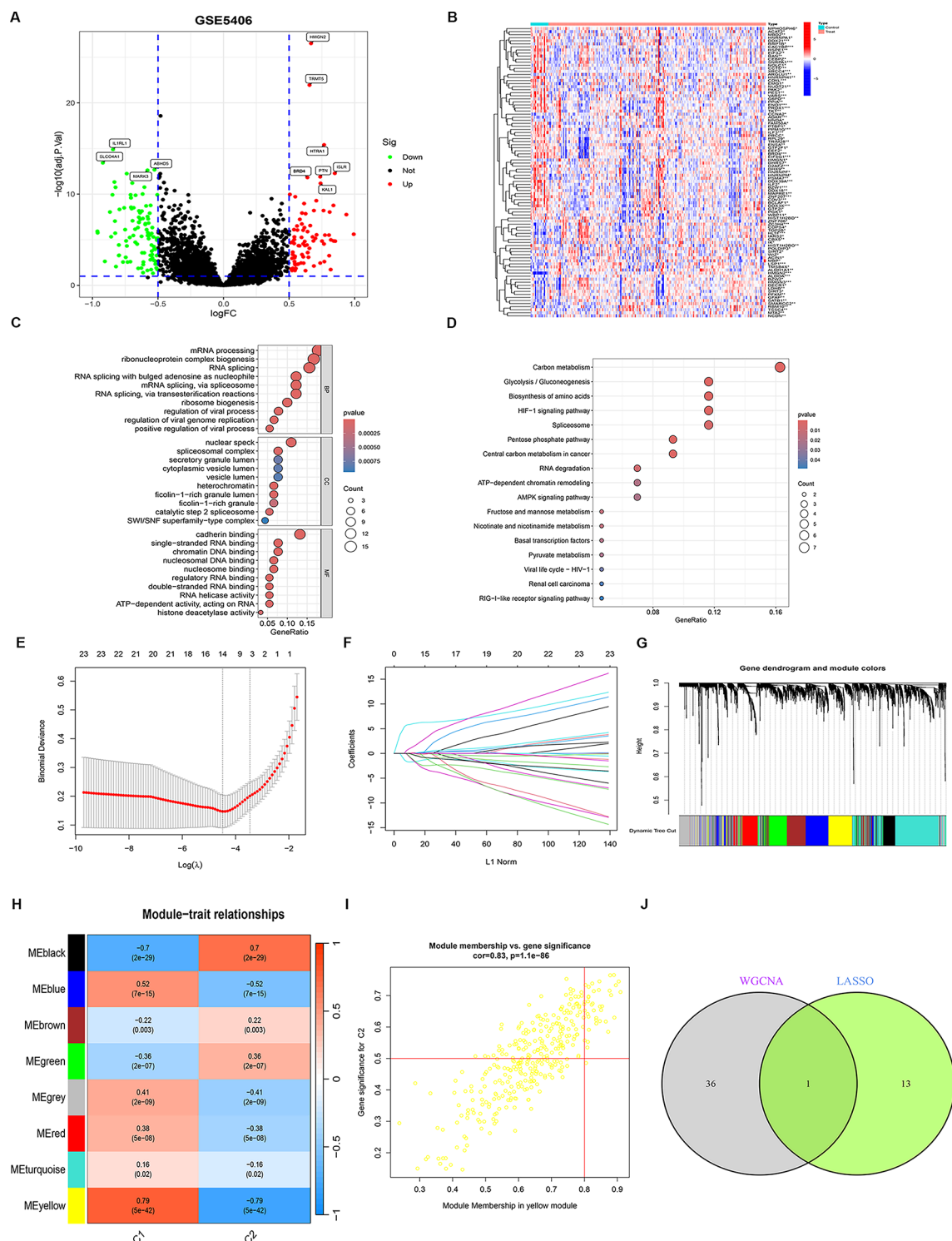


Fig. 2. Initial identification of BRD4 as a key lactonization-modified protein by machine learning. **(A–B)** Volcano and heat maps showing differentially expressed genes in the GSE5406 dataset. **(C)** GO enrichment analysis highlights the involvement of DLRGs in biological processes such as mRNA processing and ribonucleoprotein complex biogenesis, cellular components including heterochromatin, and molecular functions like nucleosomal DNA binding and cadherin binding. **(D)** KEGG pathway analysis reveals significant enrichment of DLRGs in pathways such as carbon metabolism, the pentose phosphate pathway, and glycolysis/gluconeogenesis. **(E–F)** LASSO analysis results identifying 14 key DLRGs: BRD4, CCNA2, CDV3, CDYL, H2AFZ, HIST1H2BO, HLTf, HMGN2, LSP1, MBD2, NCDN, RBM10, TMSB4X and ZNF207. **(G)** The WGCNA identifying 8 distinct gene modules. **(H–I)** Positive correlation analysis showing a significant association between the MEyellow module and HF, identifying 37 key genes. **(J)** Venn diagram illustrating the intersection of key genes identified by LASSO and WGCNA analyses, highlighting BRD4 as the potential key DLRG.

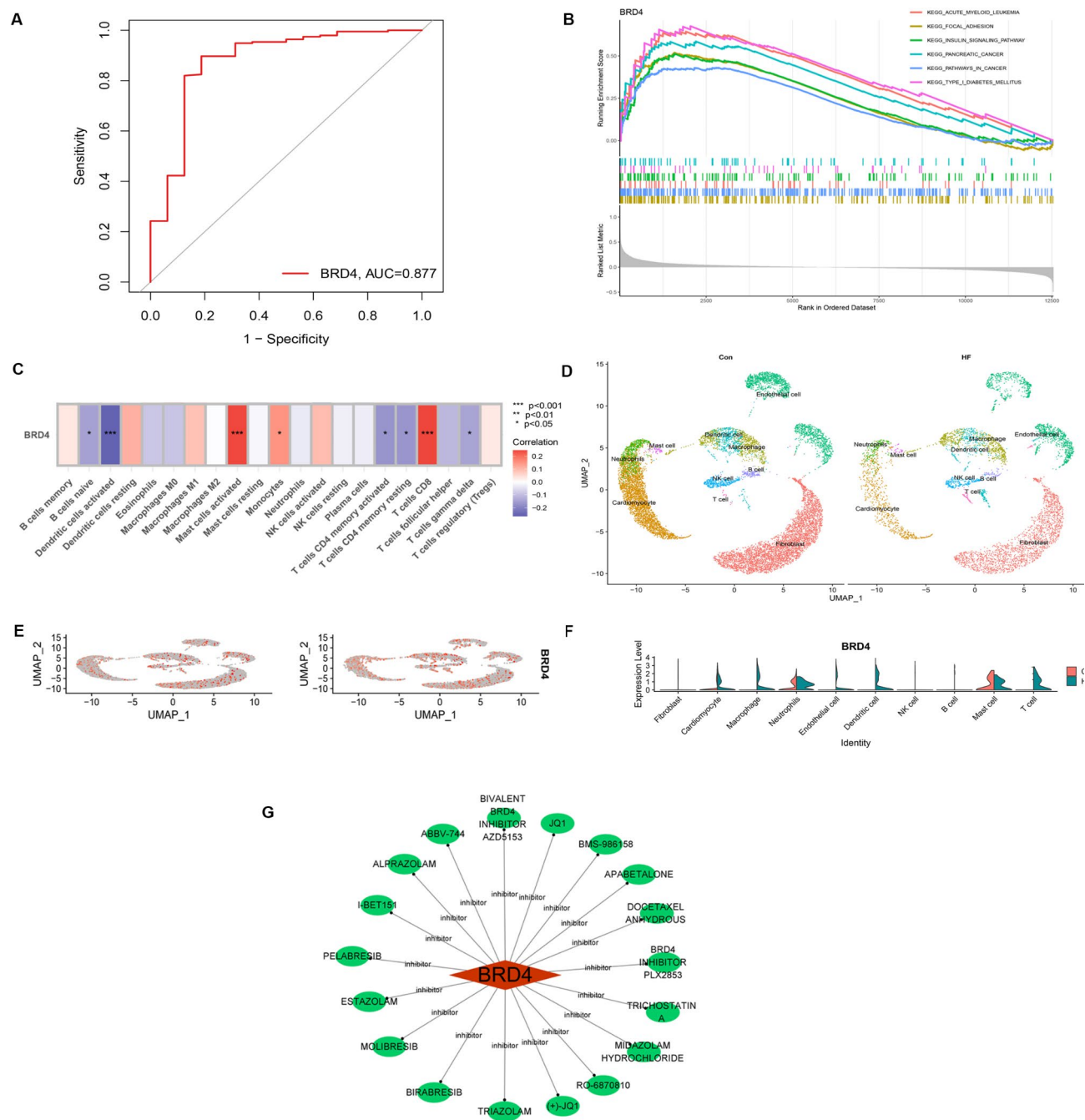


Fig. 3. Identification of BRD4 as the key gene and its association with HF pathways and immune cell infiltration. **(A)** The ROC curve analysis showing that the BRD4 gene has an Area Under the Curve score of 0.877, indicating high diagnostic accuracy and reliability in HF. **(B)** The GSEA indicating that BRD4 is closely associated with pathways such as focal adhesion, pathways in cancer, and the acute insulin signaling pathway. **(C)** Correlation analysis of BRD4 expression levels with immune cell activation, demonstrating a positive correlation with mast cell activation and T cells CD8, and a negative correlation with dendritic cell activation and T cells CD4 activation ($P < 0.05$ for all). **(D)** Ten cell types were identified using the top 10 subtype-specific DEGs: B cells, cardiomyocytes, dendritic cells, endothelial cells, fibroblasts, macrophages, mast cells, neutrophils, NK cells, and T cells. **(E-F)** BRD4 was highly expressed in cardiomyocytes, macrophages, neutrophils, dendritic cells, T cells, and mast cells. In the HF group, BRD4 expression was significantly increased in cardiomyocytes, dendritic cells, and T cells compared to the control group. **(G)** 19 potential drugs targeting BRD4 were predicted through DGIdb database.

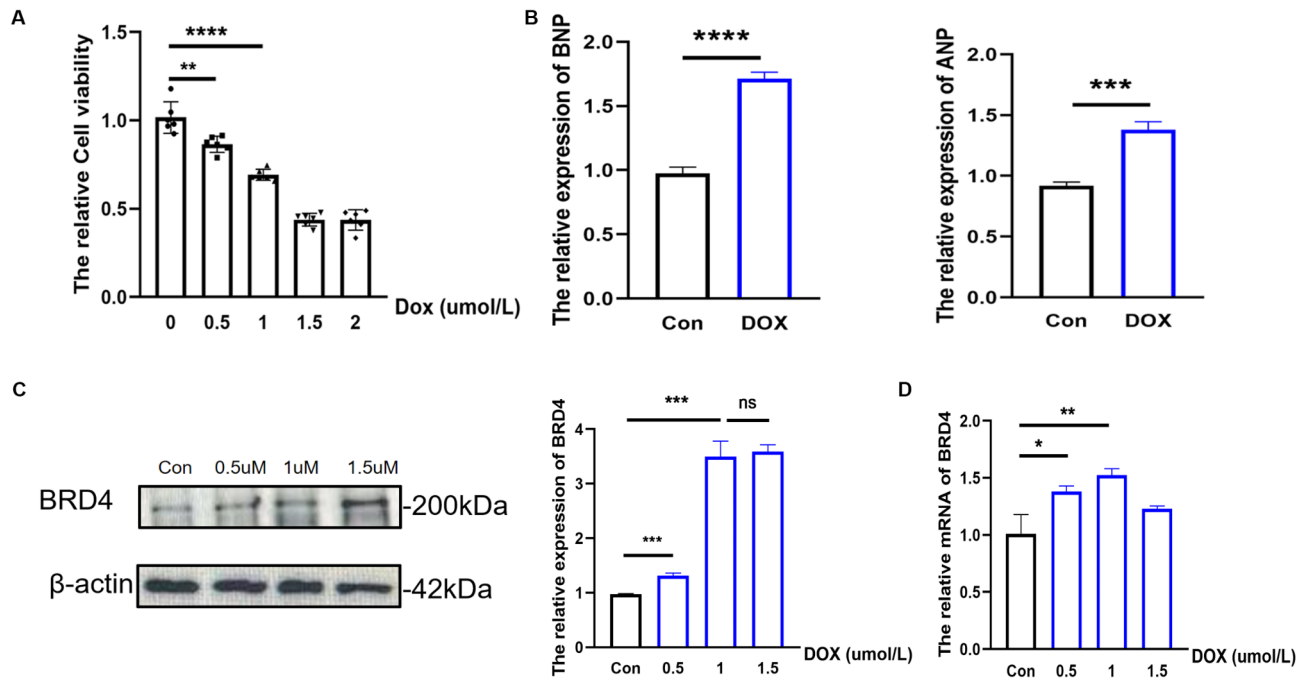


Fig. 4. Construction of in vitro HF cell model and analysis of BRD4. **(A)** Cell viability assay using CCK8 after treating AC16 cells with different concentrations of DOX (0.5 μmol/L, 1 μmol/L, 1.5 μmol/L, and 2 μmol/L). Results indicate a significant decrease in AC16 cell viability with increasing DOX concentrations, with viability at approximately 75% at 1 μmol/L DOX and significantly decreasing to around 50% at 1.5 μmol/L DOX. **(B)** mRNA expression levels of BNP and ANP in the heart failure cell model treated with 1 μmol/L DOX, showing significant elevation compared to the control group, confirming successful model construction. **(C)** Western blot analysis of BRD4 protein expression in the heart failure cell model, demonstrating an increase in BRD4 protein levels with higher DOX concentrations. **(D)** Quantitative PCR analysis of BRD4 mRNA expression in the heart failure cell model, indicating elevated BRD4 mRNA levels compared to the control group.

significant decrease in AC16 cell viability with increasing DOX concentrations (Fig. 4A). Cell viability was approximately 75% at 1 μmol/L DOX and significantly decreased to around 50% at 1.5 μmol/L DOX. Thus, 1 μmol/L DOX was sufficient to simulate cardiac injury and in vitro HF^{25,26}. When compared to the control group, the mRNA expression levels of BNP and ANP were significantly elevated in the HF model, thereby confirming the successful construction of the HF cell model (Fig. 4B).

Increased protein expression of BRD4 in HF cells

The protein expression level of BRD4 in the HF cell model was detected in this study to increase with DOX concentration (Fig. 4C). When the concentration of DOX was 1 μmol/L, the BRD4 mRNA level was also increased (Fig. 4D).

Discussion

This study, through bioinformatics analysis, is the first to identify lactylation modifier genes associated with HF. Using machine learning algorithms and WGCNA, BRD4 was further pinpointed as a potential key LRGs influencing HF pathogenesis, providing novel insights for exploring the underlying mechanisms of HF.

BRD4 is a protein that recognizes and binds acetylated lysine residues on histones, facilitating the recruitment of transcriptional activators to histones, thereby promoting the expression of inflammation-related genes. Lactylation of BRD4 may enhance its transcriptional activity, leading to the upregulation of HF-associated inflammatory genes, such as pro-inflammatory cytokines and chemokines. The upregulation of these genes can exacerbate myocardial inflammatory responses and pathological cardiac remodeling²⁷. Previous studies have established the significance of BRD4 in various cardiovascular diseases. BRD4 expression has been shown to be markedly elevated in cardiac hypertrophy, where it mitigates pathological cardiac hypertrophy by reducing reactive oxygen species production and inhibiting fibrosis and inflammatory processes^{28,29}. Furthermore, BRD4 contributes to HF pathophysiology by alleviating HF-related responses through suppression of inflammatory pathways and fibrosis³⁰. In promoting myocardial fibrosis, BRD4 appears to enhance fibroblast activity and collagen synthesis³¹. Additionally, BRD4 is vital in modulating inflammatory and immune responses. Studies have demonstrated that BRD4 regulates the NF-κB signaling pathway, which is central to inflammatory responses in conditions such as cardiac hypertrophy and atherosclerosis^{32,33}.

In pathway enrichment analysis, BRD4 was closely associated with carbon metabolism, the pentose phosphate pathway, and glycolysis/glycogenesis—metabolic pathways critical for myocardial energy homeostasis. Lactylation modification of BRD4 may influence these pathways, directly impacting HF progression. Some studies suggest

that lactylation can modulate BRD4's gene-binding and activation functions, enhancing glucose utilization in cardiomyocytes and increasing lactate production, which imposes metabolic stress³⁴. Simultaneously, BRD4 may regulate key glycolytic enzymes via lactylation, resulting in lactate accumulation within the myocardium, thereby leading to acidosis and metabolic disturbances, which can impair cardiomyocyte function³⁵. Immune cell infiltration analysis indicated a positive correlation between BRD4 expression and activation of mast cells and CD8 + T cells, closely linked to inflammatory responses in HF. Research has reported that mast cell and CD8 + T cell activation promotes histamine and cytokine release. These mediators can exacerbate myocardial function by inducing cardiomyocyte injury, promoting fibrosis, and triggering further inflammatory responses³⁶. The release of cytotoxic molecules such as perforin and granzyme may directly compromise cardiomyocyte structure, contributing to adverse myocardial remodeling and functional decline.

Interestingly, this study found that BRD4 expression was decreased in heart tissue overall, but single-cell analysis revealed increased BRD4 expression in cardiomyocytes, dendritic cells, and endothelial cells. We speculate that typical mRNA microarray analyses involve mixed tissue samples containing various cell types. The overall decrease in BRD4 expression in HF patients might be due to reduced expression in most cell types, while single-cell datasets provide higher resolution, distinguishing between different cell types. The increased BRD4 expression in cardiomyocytes and dendritic cells could indicate specific response mechanisms in these cells during HF. Additionally, BRD4 may perform distinct functions in different cell types. The results showed that BRD4 was positively correlated with mast cells/CD8 + T cells, but negatively correlated with dendritic cells and CD4 + T cells. We speculate that this may reflect the dual role of BRD4 in the pathophysiology of HF. BRD4 upregulation in mast cells and cytotoxic T cells may exacerbate myocardial injury through histamine release and direct cardiomyocytes. In contrast, brd4-mediated inhibition of dendritic cell and Th2 differentiation may inhibit the antifibrotic response via STAT5, creating a vicious cycle of inflammation and remodeling^{37,38}. Notably, lactate accumulation in the failing heart may enhance lactation of BRD4, enhancing its transcriptional activity against proinflammatory targets—a hypothesis that needs to be tested in future studies.

ROC analysis showed that BRD4 had high diagnostic accuracy, suggesting that BRD4 could serve as a potential biomarker for HF, aiding diagnosis by detecting its expression levels. Future research should further explore the specific mechanisms and roles of BRD4 in HF, revealing its regulatory networks in cardiomyocytes and immune cells. Additionally, based on the mechanisms of BRD4, the development of more effective BRD4 inhibitors could be pursued to alleviate myocardial injury and inflammatory responses, with clinical trials validating their efficacy.

This study predicted 19 potential drugs that may target BRD4 using the DGIdb database. Of these, benzodiazepines such as midazolam hydrochloride and eszopiclone, although potentially brd4-targeting drugs, clinical studies have warned that benzodiazepines should not be used in heart failure due to respiratory depression and increased mortality^{39,40}. This discrepancy emphasises the need for brd4-specific inhibitors that have no off-target effects, possibly through structure-based drug design. These drugs therefore require rigorous pharmacological validation.

This study has some limitations. First, the sample size was limited, and results need to be validated in larger cohorts. Additionally, this study primarily relied on bioinformatics analysis, necessitating further in vitro and in vivo experiments to validate the roles of key genes and pathways.

Conclusion

This study identified BRD4 as a pivotal gene implicated in HF through comprehensive bioinformatics and machine learning analyses, unveiling its crucial role in distinct regulatory mechanisms within cardiomyocytes and immune cells. Our findings indicate that BRD4 may exert an influence on the progression of HF via lactylation modification, thereby underscoring its potential diagnostic and therapeutic significance in the context of HF.

Data availability

The analysis of the data set in our study GSE5406 can be obtained from the website (<https://www.ncbi.nlm.nih.gov/geo/query/acc.cgi?acc=GSE5406>). The GSE161470 can be obtained from the website (<https://www.ncbi.nlm.nih.gov/geo/query/acc.cgi?acc=GSE161470>).

Received: 20 August 2024; Accepted: 20 February 2025

Published online: 01 April 2025

References

1. Savarese, G. et al. Global burden of heart failure: a comprehensive and updated review of epidemiology. *Cardiovasc. Res.* **118** (17), 3272–3287 (2023).
2. Ziaeean, B. & Fonarow, G. C. Epidemiology and aetiology of heart failure. *Nat. Rev. Cardiol.* **13** (6), 368–378 (2016).
3. Obokata, M. et al. Epidemiology, pathophysiology, diagnosis, and therapy of heart failure with preserved ejection fraction in Japan. *J. Card Fail.* **29** (3), 375–388 (2023).
4. Boersma, E. M. et al. Congestion in heart failure: a contemporary look at physiology, diagnosis and treatment. *Nat. Rev. Cardiol.* **17** (10), 641–655 (2020).
5. Fan, H. et al. Lactylation: novel epigenetic regulatory and therapeutic opportunities. *Am. J. Physiol. Endocrinol. Metab.* **324** (4), E330–E338 (2023).
6. Xin, Q. et al. Lactylation: a passing fad or the future of posttranslational modification. *Inflammation* **45** (4), 1419–1429 (2022).
7. Wang, N. et al. Histone lactylation boosts reparative gene activation Post-Myocardial infarction. *Circ. Res.* **131** (11), 893–908 (2022).
8. Fan, M. et al. Lactate promotes endothelial-to-mesenchymal transition via Snail1 lactylation after myocardial infarction. *Sci. Adv.* **9** (5), eadc9465 (2023).
9. Yu, W. et al. HSPA12A maintains aerobic glycolytic homeostasis and Histone3 lactylation in cardiomyocytes to attenuate myocardial ischemia/reperfusion injury. *JCI Insight* **9**(7). (2024).

10. Wang, Y. et al. Exercise-induced endothelial Mecp2 lactylation suppresses atherosclerosis via the Ereg/MAPK signalling pathway. *Atherosclerosis* **375**, 45–58 (2023).
11. Zhang, Y. et al. Macrophage MCT4 Inhibition activates reparative genes and protects from atherosclerosis by histone H3 lysine 18 lactylation. *Cell. Rep.* **43** (5), 114180 (2024).
12. Huang, H. et al. A multi-dimensional approach to unravel the intricacies of lactylation related signature for prognostic and therapeutic insight in colorectal cancer. *J. Transl Med.* **22** (1), 211 (2024).
13. Cheng, Z. et al. Lactylation-Related gene signature effectively predicts prognosis and treatment responsiveness in hepatocellular carcinoma. *Pharmaceuticals (Basel)* **16**(5). (2023).
14. Kanehisa, M., Furumichi, M., Sato, Y., Ishiguro-Watanabe, M. & Tanabe, M. KEGG: integrating viruses and cellular organisms. *Nucleic Acids Res.* **49** (D1), D545–D551 (2021).
15. Gene Ontology, C. Gene ontology consortium: going forward. *Nucleic Acids Res.* **43** (Database issue), D1049–1056 (2015).
16. Li, Y., Lu, F. & Yin, Y. Applying logistic LASSO regression for the diagnosis of atypical Crohn's disease. *Sci. Rep.* **12** (1), 11340 (2022).
17. Mandrekar, J. N. Receiver operating characteristic curve in diagnostic test assessment. *J. Thorac. Oncol.* **5** (9), 1315–1316 (2010).
18. Yu, G., Wang, L. G., Han, Y. & He, Q. Y. ClusterProfiler: an R package for comparing biological themes among gene clusters. *OMICS* **16** (5), 284–287 (2012).
19. Tu, X., Huang, H., Xu, S., Li, C. & Luo, S. Single-cell transcriptomics reveals immune infiltrate in sepsis. *Front. Pharmacol.* **14**, 1133145 (2023).
20. Chen, G., Ning, B. & Shi, T. Single-Cell RNA-Seq technologies and related computational data analysis. *Front. Genet.* **10**, 317 (2019).
21. Yu, L. et al. Characterization of cancer-related fibroblasts (CAF) in hepatocellular carcinoma and construction of CAF-based risk signature based on single-cell RNA-seq and bulk RNA-seq data. *Front. Immunol.* **13**, 1009789 (2022).
22. Luecken, M. D. & Theis, F. J. Current best practices in single-cell RNA-seq analysis: a tutorial. *Mol. Syst. Biol.* **15** (6), e8746 (2019).
23. Xu, Z. et al. Liquiritigenin alleviates doxorubicin-induced chronic heart failure via promoting ARHGAP18 and suppressing RhoA/ROCK1 pathway. *Exp. Cell. Res.* **411** (2), 113008 (2022).
24. Li, H. et al. Daidzein alleviates doxorubicin-induced heart failure via the SIRT3/FOXO3a signaling pathway. *Food Funct.* **13** (18), 9576–9588 (2022).
25. Zhang, Q., Li, J., Peng, S., Zhang, Y. & Qiao, Y. Rosmarinic acid as a candidate in a phenotypic profiling Cardio-/Cytotoxicity cell model induced by doxorubicin. *Molecules* **25**(4). (2020).
26. Reis-Mendes, A. et al. Comparative in vitro study of the cytotoxic effects of doxorubicin's main metabolites on cardiac AC16 cells versus the parent drug. *Cardiovasc. Toxicol.* **24** (3), 266–279 (2024).
27. Zheng, B. et al. Distinct layers of BRD4-PTEFb reveal bromodomain-independent function in transcriptional regulation. *Mol. Cell.* **83** (16), 2896–2910e2894 (2023).
28. Zhu, W. et al. BRD4 blockage alleviates pathological cardiac hypertrophy through the suppression of fibrosis and inflammation via reducing ROS generation. *Biomed. Pharmacother.* **121**, 109368 (2020).
29. Huang, C. et al. Up-regulation of BRD4 contributes to gestational diabetes mellitus-induced cardiac hypertrophy in offspring by promoting mitochondria dysfunction in sex-independent manner. *Biochem. Pharmacol.* **226**, 116387 (2024).
30. Duan, Q. et al. BET bromodomain Inhibition suppresses innate inflammatory and profibrotic transcriptional networks in heart failure. *Sci. Transl Med.* **9**(390). (2017).
31. Song, S. et al. BRD4 as a therapeutic target for atrial fibrosis and atrial fibrillation. *Eur. J. Pharmacol.* **977**, 176714 (2024).
32. Li, X. et al. Non-canonical STING-PERK pathway dependent epigenetic regulation of vascular endothelial dysfunction via integrating IRF3 and NF-kappaB in inflammatory response. *Acta Pharm. Sin. B.* **13** (12), 4765–4784 (2023).
33. Fang, M., Luo, J., Zhu, X., Wu, Y. & Li, X. BRD4 Silencing protects angiotensin II-Induced cardiac hypertrophy by inhibiting TLR4/NF-kappaB and activating Nrf2-HO-1 pathways. *Cardiol. Res. Pract.* **2022**, 8372707 (2022).
34. Monteith, A. J. et al. Lactate utilization enables metabolic escape to confer resistance to BET Inhibition in acute myeloid leukemia. *Cancer Res.* **84** (7), 1101–1114 (2024).
35. Modi, N. et al. BRD4 regulates Glycolysis-Dependent Nos2 expression in macrophages upon H pylori infection. *Cell. Mol. Gastroenterol. Hepatol.* **17** (2), 292–308 (2024). e291.
36. Chen, Y., Griffiths, C. E. M. & Bulfone-Paus, S. Exploring mast cell-CD8 T cell interactions in inflammatory skin diseases. *Int. J. Mol. Sci.* **24**(2). (2023).
37. Milner, J. J. et al. Bromodomain protein BRD4 directs and sustains CD8 T cell differentiation during infection. *J. Exp. Med.* **218**(8). (2021).
38. Yu, J. et al. Progestogen-driven B7-H4 contributes to onco-fetal immune tolerance. *Cell* **187** (17), 4713–4732e4719 (2024).
39. Ribeirinho-Soares, P. et al. Benzodiazepine use and mortality in chronic heart failure. *Pol. Arch. Intern. Med.* **133**(10). (2023).
40. Chuang, C. et al. Benzodiazepines in patients with heart failure and reduced ejection fraction. *Acta Cardiol. Sin.* **38** (5), 573–583 (2022).

Acknowledgements

None.

Author contributions

This study was designed by KL and LH. KL, ZZ and MS contributed to the data collection and analysis. KL and XW wrote the first draft of the paper. JY and LZ revised the article. All authors read and approved the final manuscript.

Funding

This work was supported by Clinical Specialist Talents' Professional Ability Innovation and Application Research Project (No. RCLX2315029), 2022 Taizhou Science and Technology Support Program (Social Development) Project (No. TS202219).

Declarations

Competing interests

The authors declare no competing interests.

Additional information

Supplementary Information The online version contains supplementary material available at <https://doi.org/10.1038/s41598-025-91506-x>

[0.1038/s41598-025-91506-x](https://doi.org/10.1038/s41598-025-91506-x).

Correspondence and requests for materials should be addressed to J.Y. or L.Z.

Reprints and permissions information is available at www.nature.com/reprints.

Publisher's note Springer Nature remains neutral with regard to jurisdictional claims in published maps and institutional affiliations.

Open Access This article is licensed under a Creative Commons Attribution-NonCommercial-NoDerivatives 4.0 International License, which permits any non-commercial use, sharing, distribution and reproduction in any medium or format, as long as you give appropriate credit to the original author(s) and the source, provide a link to the Creative Commons licence, and indicate if you modified the licensed material. You do not have permission under this licence to share adapted material derived from this article or parts of it. The images or other third party material in this article are included in the article's Creative Commons licence, unless indicated otherwise in a credit line to the material. If material is not included in the article's Creative Commons licence and your intended use is not permitted by statutory regulation or exceeds the permitted use, you will need to obtain permission directly from the copyright holder. To view a copy of this licence, visit <http://creativecommons.org/licenses/by-nc-nd/4.0/>.

© The Author(s) 2025